Kink-breather solution in the weakly discrete Frenkel-Kontorova model

S. V. Dmitriev,* T. Miyauchi, K. Abe, and T. Shigenari
Department of Applied Physics and Chemistry, University of Electro-Communications, Chofu-shi, Tokyo 182-8585, Japan
(Received 9 November 1999)

The discrete Frenkel-Kontorova model, having the sine-Gordon equation as the continuous analog, was investigated numerically at a small degree of discreteness. Interaction between a kink and a breather in a discrete system was compared with the exact three-soliton solution to the continuous sine-Gordon equation. Nontrivial effects of discreteness were found numerically. One is that a kink and a breather in the discrete system are mutually attractive quasiparticles, so they can be regarded as a three-soliton oscillatory system. The other is the energy exchange between a kink and a breather when their collision takes place in a vicinity of a separatrix solution to the continuous sine-Gordon equation. We have estimated numerically the kink-breather binding energy E_B and the maximum possible exchange energy E_E for different breather frequencies ω. The results suggest that there is a threshold breather frequency for the ''spontaneous'' breaking up of the three-soliton oscillatory system into a kink and a breather moving in opposite directions.

PACS number(s): 41.20.Jb, 36.20.−r, 45.05.+x, 63.20.Ry

I. INTRODUCTION

The sine-Gordon (SG) equation appears in many different fields of physics [1–3]. In each field the SG equation is usually considered with some distinctive perturbation terms [4–7]. For example, in solid state physics, the discreteness of media at a microscopic level makes it important to study the discrete form of the SG equation, which is the Frenkel-Kontorova model [8].

The discreteness effect on the one- and two-soliton SG solutions has been extensively studied, see the review by Braun and Kivshar [9], references therein and also [10–14]. For many-soliton solutions (more than two) a new effect of perturbation has been found, namely, the energy exchange between solitons [4,15–18]. It has been demonstrated that the separatrix solutions to the SG equation are responsible for this effect [16].

In the vicinity of a separatrix solution, even a small perturbation can have a pronounced effect on the dynamics of the system [19,20]. This is also true for the particular case of the SG equation perturbed by the discreteness. In this paper, we show that the effect of discreteness can be noticeable even for a weak discreteness ($h<0.5$, for the definition of h see below), when all other manifestations of discreteness are very small.

In Sec. II, for the sake of convenience, we reproduce the results of Ref. [16] describing the kink-breather SG solution and a separatrix three-soliton solution. In Sec. III, we give some details of the numerical investigation. In Sec. IV, we demonstrate numerically the possibility of energy exchange between a kink and a breather in the weakly discrete SG system. In Sec. V, we discuss the numerical results of the kink-breather mutual attraction study.

II. FRENKEL-KONTOROVA MODEL AND SG EQUATION

We consider the Hamiltonian of the Frenkel-Kontorova model [8] in a dimensionless form

$$H=\sum_n E_n=\sum_n \left[\frac{p_n^2}{2}+\frac{1}{2h^2}(u_{n+1}-u_n)^2+(1-\cos u_n)\right], \tag{1}$$

where E_n is the energy of nth particle, u_n is the displacement of the particle from an initial point with coordinate $x=nh$, p_n is the momentum of the particle with a unit mass, H/h is the density of energy, and h is the only parameter of the system, which gives a measure of discreteness because the equations of motion obtained from the Hamiltonian Eq. (1),

$$\frac{d^2u_n}{dt^2}-\frac{1}{h^2}(u_{n-1}-2u_n+u_{n+1})+\sin u_n=0, \tag{2}$$

in the continuum limit $(h\rightarrow 0)$, are reduced to the SG equation

$$u_{tt}-u_{xx}+\sin u=0. \tag{3}$$

Many-soliton solutions to Eq. (3) can be derived by means of the Hirota method [21] or by the Bäcklund transformation (see, e.g., [2]).

The three-soliton solution to Eq. (3), which describes the collision between a kink and a breather, has been reported in Ref. [16] in the following form

$$u=v+w. \tag{4}$$

The function v is the kink solution

$$v=4\arctan\exp B, \tag{5}$$

where $B=\delta_k(x-x_k-d_k t)$, $0\leqslant d_k<1$ is the velocity of the kink, $\delta_k^{-1}=\sqrt{1-d_k^2}$, and x_k defines the position of the kink at the time $t=0$.

The second part of the solution Eq. (4) is

$$w=4\arctan[(\eta X)/(\omega Y)], \tag{6}$$

with

*Permanent address: General Physics Department, Barnaul State Technical University, 46, Lenin Street, 656099, Barnaul, Russia.

$$X=2\omega(\sinh D-\cos C\sinh B)+2\delta_k\delta_b(d_k-d_b)\sin C\cosh B, \tag{7}$$

$$Y=2\eta(\cos C+\sinh D\sinh B)-2\delta_k\delta_b(1-d_kd_b)\cosh D\cosh B, \tag{8}$$

where $C=-\omega\delta_b[t-d_b(x-x_b)]+2\pi m$ with an integer m, $D=\eta\delta_b(x-x_b-d_bt)$, $0\leqslant d_b<1$ is the velocity of the breather, $\delta_b^{-1}=\sqrt{1-d_b^2}$, $0\leqslant\omega<1$ is the frequency of the breather, $\eta=\sqrt{1-\omega^2}$, x_b defines the position of the breather at the time $t=0$.

In the continuum limit the velocity of the breather d_b, its wavelength λ, and period T are related to each other by the following expressions:

$$|d_b|=\lambda/T,\quad \lambda=2\pi\delta_b|d_b|/\omega,\quad T=2\pi\delta_b/\omega. \tag{9}$$

The amplitude A and the energy E_b of the breather are

$$A=4\arctan(\eta/\omega),\quad E_b=16\eta\delta_b. \tag{10}$$

The energy of the kink is $E_k=8\delta_k$ and the energy of the solution (4) is $E=E_k+E_b$.

The masses of the kink and the breather are

$$M_k=8\delta_k=E_k,\quad M_b=16\eta\delta_b=E_b. \tag{11}$$

The widths of the kink and the breather can be defined as

$$W_k=\delta_k^{-1},\quad W_b=(\eta\delta_b)^{-1}. \tag{12}$$

For $d_k=0$, $W_k=1$. The width of the kink gives the notion of the discreteness parameter h, which should be viewed in comparison with W_k.

Collision between a kink and a breather results in the phase shifts that, in non-relativistic limit, can be expressed as follows:

$$\Delta_k=4\tanh^{-1}\eta,\quad \Delta_b=\frac{2}{\eta}\tanh^{-1}\eta. \tag{13}$$

The coordinate and the time of collision of the kink with the center of mass of the breather are

$$x_c=\frac{d_kx_b-d_bx_k}{d_k-d_b},\quad t_c=\frac{x_b-x_k}{d_k-d_b}. \tag{14}$$

If $d_k=d_b$ then, for $x_k\neq x_b$, the kink never passes through the center of mass of the breather and, for $x_k=x_b$, the kink constantly locates at the center of mass of the breather.

Note that the center of kink in the solution Eq. (4) is not located at x_k; and that the center of the breather is not at x_b. Far from the collision point, before and after the collision, the center of the kink or breather moves in the (x,t) plane along the lines

$$x-x_c\pm\frac{\Delta}{2}=d(t-t_c), \tag{15}$$

where Δ and d are the phase shift and the velocity of kink or breather, respectively.

If

$$\omega(x_b-x_k)=2\pi m\delta_b(d_k-d_b), \tag{16}$$

where m is an integer, then at $t=t_c$ all three kinks collide at one point $x=x_c$.

Equation (4) subjected to the condition Eq. (16) and to the condition

$$(d_k-d_b)\to 0 \tag{17}$$

is a separatrix three-soliton solution to the SG equation.

Note, that the condition Eq. (17) generalizes the condition $d_k\to 0$ and $d_b\to 0$ given in Ref. [16]. The generalization can be easily done with the help of the Lorentz transformation.

III. MOLECULAR DYNAMICS SIMULATION

Equation (4) predicts the purely elastic interaction between quasiparticles with no energy exchange between them or radiation. Here we study the influence of a weak discreteness on the three-soliton solution.

Equations of motion of the Frenkel-Kontorova model, Eq. (2), were integrated numerically. We rewrite Eq. (2) in the form

$$\ddot{u}_n=R_n, \tag{18}$$

where $R_n=(u_{n-1}-2u_n+u_{n+1})/h^2-\sin u_n$ and introduce the time mesh $t_j=j\Delta t$, $j=0,1,2,\ldots$ with the time step Δt. By the Störmer method of order six [22] the unknown functions $u_n(t)$ at the $(j+1)$th time step can be found as

$$u_{n,j+1}=2u_{n,j}-u_{n,j-1}+\Delta t^2\left(\frac{7}{6}R_{n,j}-\frac{5}{12}R_{n,j-1}+\frac{1}{3}R_{n,j-2}-\frac{1}{12}R_{n,j-3}\right). \tag{19}$$

When calculating the kinetic energy of a particle we used the following approximation for the velocity

$$\dot{u}_{n,j}=\frac{2u_{n,j}+3u_{n,j-1}-6u_{n,j-2}+u_{n,j-3}}{6\Delta t}. \tag{20}$$

For the time step we put $\Delta t=10^{-3}$. The numerical data reported in this paper did not vary essentially with further decreasing of Δt.

The solution Eq. (4) to the continuous equation Eq. (3), after the substitution $x\to nh$ and $t\to j\Delta t$, was used for setting the initial conditions for the discrete system Eq. (2).

A kind of absorbing boundary conditions for the chain containing 401 particles $(-200\leqslant n\leqslant 200)$ was used in order to exclude the influence of the radiation reflected from the boundaries. For the discreteness parameter we set $h=0.2$ (weak discreteness).

IV. ENERGY EXCHANGE BETWEEN KINK AND BREATHER

Let us first study the influence of the weak discreteness $(h=0.2)$ on the kink-breather collision. For this study we put the breather frequency $\omega=0.3$; the velocities of the kink and the breather $d_k=0$, $d_b=-0.2$; the kink position parameter

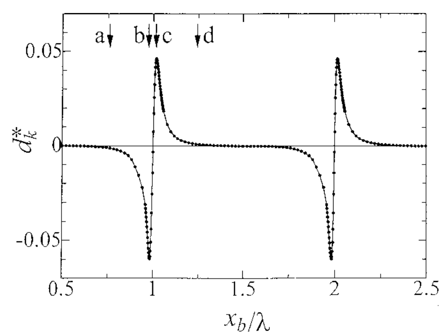

FIG. 1. Velocity of the kink after the collision d_k^* as the function of the phase of collision x_b/λ. The inelasticity of collision, presented by d_k^*, drastically increases in the vicinity of $x_b/\lambda = m$.

$x_k = 0$ and different magnitudes for the breather position parameter $x_b > 0$.

According to the choice of parameters, before the collision kink is at rest, the breather moves toward the kink from the right to the left. The breather moves in an oscillatory manner and, as it has been demonstrated in Ref. [16], the inelasticity of the kink-breather collision strongly depends on the phase at which the breather meets the kink. Variation of x_b means the variation of the phase of collision. The velocity of the kink after the collision d_k^* is a suitable measure of inelasticity of the kink-breather interaction. The velocity d_k^* was determined when the kink was far from the breather after the collision.

In Fig. 1, the inelasticity of collision d_k^* is presented as the function of the phase of collision x_b/λ, where λ is given by Eq. (9). Obviously, the function $d_k^*(x_b/\lambda)$ should have the period equal to unity. As Fig. 1 suggests, the inelasticity of collision drastically increases in the vicinity of $x_b/\lambda = m$. One can easily check that the condition $x_b/\lambda = m$ coincides with the condition of separatrix solution Eq. (16) at $x_k = 0$ and $d_k = 0$, considered in our numerical example. The second condition of the separatrix solution, Eq. (17), is also nearly fulfilled because $d_k - d_b = 0.2$, which is sufficiently small.

In Figs. 2(a)–2(d), we show the kink-breather collisions at different phases of collision, shown in Fig. 1 by the corresponding arrows. The particles of the chain having energy $E_n \geqslant 0.5$ [see Eq. (1)] are shown in Fig. 2 by black dots and the particles with energy $E_n < 0.5$ are not shown. Thus, the black areas show the cores of solitons having a high energy. In Figs. 2(a) and 2(d) collision takes place far from separatrix and it is nearly elastic. In Figs. 2(b) and 2(c) all three kinks collide practically at one point and with a small relative velocity or, in other words, the conditions of the separatrix solution, Eq. (16) and Eq. (17), are nearly fulfilled. Collision in the vicinity of separatrix is inelastic.

V. ATTRACTION BETWEEN KINK AND BREATHER

For this study we set the parameters as follows: Discreteness parameter $h = 0.2$; breather frequency $\omega = 0.2$, 0.3, and 0.4; velocities of the kink and the breather $d_k = d_b = 0$; the breather position parameter $x_b = 0$, and different magnitudes for the kink position parameter x_k. The difference $x_k - x_b$ and the phase shifts Δ_k and Δ_b define the distance between the centers of the kink and the breather. We study the case of

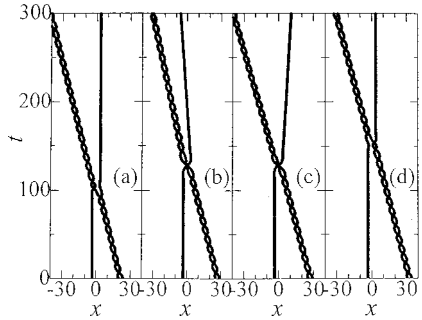

FIG. 2. Time evolution of the kink-breather collisions at different phases of collision. Arrows in Fig. 1 show the phases of collision for (a)–(d), respectively. The particles of the chain having energy $E_n \geqslant 0.5$ are shown by black dots and the particles with energy $E_n < 0.5$ are not shown. Thus, the black areas show the cores of solitons. (a) and (d) Collisions take place far from the separatrix and they are nearly elastic. (b) and (c) All three kinks collide practically at one point and with a small relative velocity or, i.e., in the vicinity of the separatrix. (b) and (c) Collisions are inelastic.

small distances, when the quasiparticles overlap. We carried out the numerical integration of Eq. (2) starting from the time $t = T/4$, where the period of breather T is given by Eq. (9).

In Fig. 3, we compare the time-evolution of the discrete system Fig. 3(a) with the prediction of the continuous SG equation Fig. 3(b) for $\omega = 0.3$, $x_k = 1.2$. According to Eq. (15), at the beginning of the numerical run the center of kink locates at $x = x_k + \Delta_k/2 = 1.2 + 3.75 = 4.95$ and the center of breather locates at $x = x_b - \Delta_b/2 = 0 - 1.96 = -1.96$.

As Fig. 3(b) suggests, the overlapping breather and kink in a continuous SG system interact in such a way that for part of a period of a breather oscillation T, there is an attraction between quasiparticles and for another part of the period there is a repulsion. The attraction and the repulsion exactly compensate each other and the mean distance between quasiparticles does not vary in time. In the perturbed system [Fig. 3(a)], the attraction is not exactly compensated by the

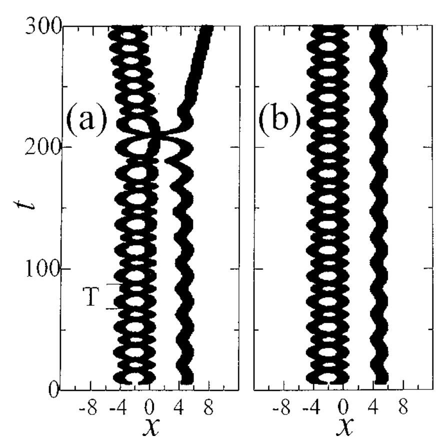

FIG. 3. (a) Time evolution of the discrete system and (b) the continuous SG equation for $\omega = 0.3$, $x_k = 1.2$. The black areas show the cores of solitons. (a) In the discrete system, the distance between quasiparticles gradually decreases due to their mutual attraction. At $t = 10T \approx 210$ (T is the period of the breather), as a result of energy exchange between quasiparticles, the three-soliton solution breaks up into a kink and a breather moving in opposite directions.

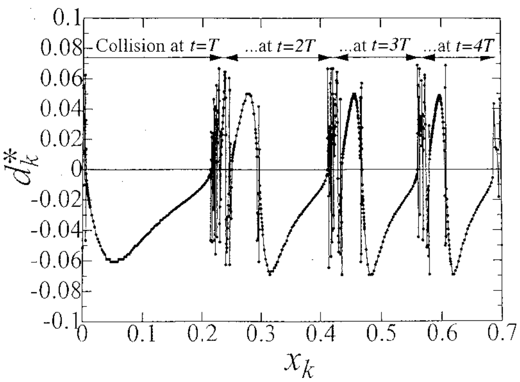

FIG. 4. Velocity of the kink after breaking up of the three-soliton solution d_k^* as the function of x_k for $\omega=0.3$.

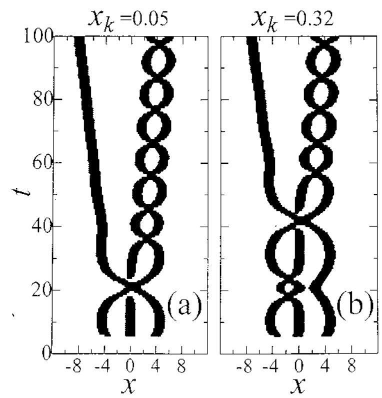

FIG. 5. Picture of breaking up of the three-soliton solution into a kink and a breather for (a) $x_k=0.05$ and (b) $x_k=0.32$.

repulsion. As a result, the distance between quasiparticles gradually decreases and at $t=10T\approx 210$, the kink collides with the breather. The collision may result in the breaking up of the three-soliton solution into a breather and a kink moving in opposite directions, as it takes place in Fig. 3(a).

The origin of the breaking up of the three-soliton solution is the energy exchange between kink and breather in the vicinity of a separatrix, as it was demonstrated in Sec. IV. If the collision is inelastic, the kink can obtain some energy and separate from the breather. The velocities of the kink and the breather after breaking up, d_k^* and d_b^*, adhere to the momentum conservation law $d_k^* M_k + d_b^* M_b = 0$, so it is enough to measure the velocity of only one particle, let us say d_k^*. We determined the velocity d_k^* numerically at a time when the kink and the breather are rather far from each other after breaking up of the three-soliton solution.

As it can be seen from Fig. 1, the velocity d_k^* is very sensitive to the ''fine structure'' of the three-soliton collision. The conditions of the three-soliton collision can be changed by the variation of the distance between kink and breather at the beginning of the numerical run, i.e., by variation of x_k (remember that we put $x_b=0$).

In Fig. 4, the velocity d_k^* is presented as the function of x_k for $\omega=0.3$. The function $d_k^*(x_k)$ is an odd function and we plot it only for $x_k \geqslant 0$. One can see the quasiperiodic character of the function, which is due to the periodic motion of the breather. Another important feature of the function $d_k^*(x_k)$ is the alternation of the regions of smooth and random behavior. The third easily observable fact is that d_k^* lies in the range $-0.07 < d_k^* < 0.07$. In the following subsections we discuss these features of the function $d_k^*(x_k)$.

A. Periodicity of $d_k^*(x_k)$

First we discuss the periodicity of the function $d_k^*(x_k)$. One must keep in mind that the kink and the breather in the discrete system are mutually attractive, so the distance between them decreases with time. In Fig. 5, we demonstrate the picture of the kink-breather collision for Fig. 5(a) $x_k = 0.05$ and Fig. 5(b) $x_k=0.32$. These two magnitudes of x_k approximately correspond to the two sequential minimums of the curve $d_k^*(x_k)$ (see Fig. 4). Actually, the distance between kink and breather at the beginning of the numerical run is equal to $x_k+\Delta_k/2+\Delta_b/2$, but for the sake of simplicity, we will drop the constant part $\Delta_k/2+\Delta_b/2$ and use x_k as the measure of the distance between quasiparticles. In Fig. 5(a), the initial distance between the kink and the breather is rather small and the collision takes place at $t=T\approx 21$, while in Fig. 5(b), the distance is larger and, at $t=T$, particles are still rather far from each other and they collide at $t=2T \approx 42$. The fine structure of collisions shown in Figs. 5(a) and 5(b) is almost the same and, consequently, the result of breaking up is similar, the kink has negative velocity in both cases. It is now clear that within the ith period of the curve $d_k^*(x_k)$, presented in Fig. 4, the collision of the three solitons takes place at $t=iT$.

The above result shows that the curve $d_k^*(x_k)$, presented in Fig. 4, gives the possibility to trace the motion of quasiparticles. Let τ be the time the quasiparticles take to reach each other due to their mutual attraction if, at the beginning of the numerical run, the distance between them is x_k and the velocities are equal to zero. The increase of x_k from one minimum (or maximum) of the curve $d_k^*(x_k)$ to the next one gives the increase of τ by T. In Fig. 6 the x_k dependence of τ/T is given by open circles for 30 successive minimums of the curve $d_k^*(x_k)$. The data were taken from Fig. 4 extended up to $x_k=2.23$.

B. Alternative behavior of $d_k^*(x_k)$

Let us turn to the discussion of the alternative behavior of the function $d_k^*(x_k)$ shown in Fig. 4. Random behavior of the function takes place when it crosses the line $d_k^*=0$. In these regions, the kink and the breather after the collision move in opposite directions with rather small velocities, not enough to overcome their mutual attraction, and quasiparticles collide again. High sensitivity of d_k^* to the x_k is responsible for the chaotic behavior of $d_k^*(x_k)$ in the case when the first collision of kink and breather does not lead to the breaking up of the three-soliton solution.

In Fig. 7, we show the time evolution of the three-soliton solution for $\omega=0.3$ and (a) $x_k=0.231$ [Fig. 7(a)], $x_k =0.296$ [Fig. 7(b)]. These two magnitudes of x_k are taken from the regions of random behavior of the function $d_k^*(x_k)$ (see Fig. 4). In Sec. V B we established the rule that within the ith period of the curve $d_k^*(x_k)$ the collision of kink and breather takes place at $t=iT$. Thus, the collision in Fig. 7(a) may have taken place at $t=T\approx 21$ or $t=2T\approx 42$ and in Fig.

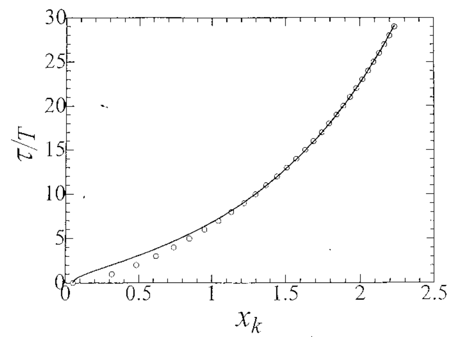

FIG. 6. Time of kink-breather collision τ in units of breather period T as a function of the initial distance between kink and breather, presented by x_k. Open circles show the x_k dependence of τ/T for 30 successive minimums of the curve $d_k^*(x_k)$ presented in Fig. 4. Solid line is the result of assumption that the attraction potential between kink and breather is given by Eq. (21) with $\alpha = 1.2\times 10^{-3}$, $R_0 = 0.52$.

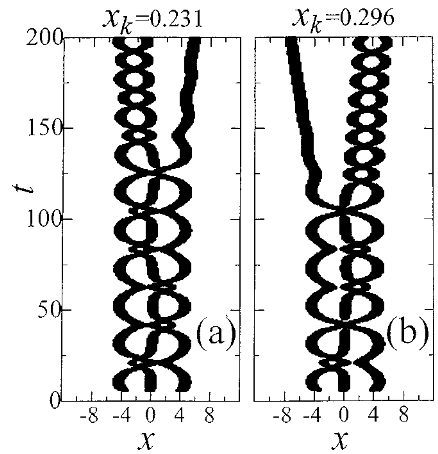

FIG. 7. Picture of breaking up of the three-soliton solution into a kink and a breather for (a) $x_k = 0.231$ and (b) $x_k = 0.296$.

7(b) at $t = 2T \approx 42$. However, energy obtained by the kink in these collisions was not big enough to overcome the attraction to the breather and hence, they collide again. The breaking up takes place in Fig. 7(a) at $6T \approx 126$ and in Fig. 7(b) at $5T \approx 105$.

C. Attraction force

We attempted to extract from the numerical data the attraction force acting between a kink and a breather. For this purpose we consider a kink and a breather as classical particles having masses M_k, M_b, coordinates $\xi_k(t)$, $\xi_b(t)$, and interacting via force

$$F(r) = \alpha \exp(-r/R_0), \tag{21}$$

where r is the distance between particles and α, R_0 are parameters. We solved numerically the equations of motion for the particles with the initial conditions $\xi_k^0 = x_k$, $\xi_b^0 = 0$, $\dot{\xi}_k^0 = 0$, $\dot{\xi}_b^0 = 0$. We calculated the time τ of collision of the particles as a function of x_k. The goal of the calculation was to fit, by proper choice of α and R_0, the data shown in Fig. 6 by open circles. The result for $\alpha = 1.2\times 10^{-3}$, $R_0 = 0.52$, is shown in Fig. 6 by a solid line.

As can be seen from Fig. 6, the exponential law for the force Eq. (21) is valid for a not very small distance between kink and breather ($x_k > 1.0$). For $x_k < 1.0$, Fig. 6 suggests that the actual attraction force between kink and breather is greater than that predicted by the approximation Eq. (21). What actually happens is the acceleration of quasiparticles due to the energy exchange, which takes place at small x_k or, in other words, in the vicinity of separatrix.

D. Influence of ω

So far the case of the breather's frequency $\omega = 0.3$ has been studied. Similar numerical results were obtained for $\omega = 0.2$ and 0.4. Let us discuss the influence of ω on the behavior of the three-soliton solution.

There are two factors that define the behavior of the three-soliton solution. The first stabilizing factor is the binding energy of kink and breather

$$E_B = \int_0^\infty F(r)\,dr = \alpha R_0. \tag{22}$$

The three-soliton solution breaks up due to the energy exchange between solitons. The energy obtained by kink in the form of kinetic energy is equal to the reduction of the breather's energy (for the case of weak discreteness one can neglect the radiation losses). Thus, the second, destructive factor is the maximum exchange energy E_E, i.e., the maximum kinetic energy of the kink after breaking up

$$E_E = \frac{1}{2} M_k (\max|d_k^*|)^2. \tag{23}$$

If $E_E < E_B$ then the three-soliton solution cannot break up because the kink cannot obtain from the breather the amount of energy sufficient to escape. For example, for $\omega = 0.3$ one has $E_B = 6.2\times 10^{-4}$, and $E_E = 0.02$, where we used $M_k = 8$ and $\max|d_k^*| = 0.07$ (see Fig. 4). Similar data for different magnitudes of ω are given in Table I.

It is interesting to compare the binding energy of kink and breather E_B with the maximum exchange energy E_E for different ω. The comparison is given in Fig. 8. As may be seen, the ratio E_E/E_B decreases rapidly with increase in ω (note the logarithmic scale for the ordinate). From the extrapola-

TABLE I. Numerical data for different ω.

ω	α	R_0	E_B	$\max\|d_k^*\|$	E_E	E_E/E_B
0.2	2.8×10^{-4}	0.53	1.5×10^{-4}	0.12	5.8×10^{-2}	390
0.3	1.2×10^{-3}	0.52	6.2×10^{-4}	0.07	2.0×10^{-2}	32
0.4	3.7×10^{-3}	0.46	1.7×10^{-3}	0.04	6.4×10^{-3}	3.8

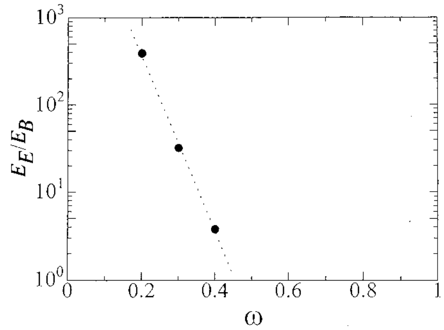

FIG. 8. Ratio E_E/E_B as the function of ω. For a small ω, the exchange energy E_E is greater than the binding energy E_B. The extrapolation (the dotted line) suggests that in the region of large ω ($\omega > 0.5$) the three-soliton oscillatory system cannot break up because, in that region, E_B is larger than E_E.

tion, one would expect that for large ω the binding energy E_B should be greater than the exchange energy E_E, which is to say that the three-soliton solution cannot break up. More precisely, breaking up takes place but the kinetic energy obtained by quasiparticles is not enough to overcome their mutual attraction and they cannot separate from each other, they should collide again and again.

We checked numerically the last conclusion. For $\omega = 0.6$ the breaking up of the three-soliton solution was not observed up to $t = 10^3 T$ at different x_k. Most likely for $h = 0.2$ and $\omega \geqslant 0.6$ the kink and the breather can create a stable three-soliton quasiparticle that never breaks up into a kink and a breather.

VI. CONCLUSION

A new effect of discreteness on the three-soliton SG solution, namely, the attraction between a kink and a breather, was found numerically. This attraction binds the kink and the breather into a three-soliton oscillatory system.

The three-soliton oscillatory system shows the effect of instability. We attribute this effect to the energy exchange between solitons that can take place in the vicinity of the separatrix three-soliton solution to the SG equation [16].

Comparison of the binding energy E_B for a kink and a breather with the maximum exchange energy E_E revealed that E_E is larger than E_B for small ω. Meanwhile, it is expected from the extrapolation that, for large ω, E_E cannot exceed E_B. Consequently, it appears that the three-soliton oscillatory system with small ω can spontaneously break up into a kink and a breather moving in opposite directions. For a large ω the three-soliton oscillatory system never breaks up.

ACKNOWLEDGMENTS

One of the authors (S.V.D.) wishes to thank the Japan Society for the Promotion of Science for their financial support.

[1] M. Remoissenet, *Waves Called Solitons* (Springer, Berlin-Heidelberg, 1994).

[2] R. K. Dodd, J. C. Eilbeck, J. D. Gibbon, and H. C. Morries, *Solitons and Nonlinear Wave Equations* (Academic Press, London, 1982).

[3] A. S. Davydov, *Solitons in Molecular Systems* (Reidel, Dordrecht, 1985).

[4] Yu. S. Kivshar and B. A. Malomed, Rev. Mod. Phys. **61**, 763 (1989).

[5] N. R. Quintero and A. Sánchez, Eur. Phys. J. B **6**, 133 (1998).

[6] Yu. S. Kivshar, F. Zhang, and L. Vázquez, Phys. Rev. Lett. **67**, 1177 (1991).

[7] A. Kwaśniewski, P. Machnikowski, and P. Magnuszewski, Phys. Rev. E **59**, 2347 (1999).

[8] T. Kontorova and Ya. T. Frenkel, Zh. Eksp. Teor. Fiz. **8**, 1340 (1938).

[9] O. M. Braun and Yu. S. Kivshar, Phys. Rep. **306**, 1 (1998).

[10] T. R. Koehler, A. R. Bishop, J. A. Krumhansl, and J. R. Schrieffer, Solid State Commun. **17**, 1515 (1975).

[11] S. Aubry, J. Chem. Phys. **64**, 3392 (1976).

[12] S. E. Trullinger, M. D. Miller, R. A. Guyer, A. R. Bishop, F. Palmer, and J. A. Krumhansl, Phys. Rev. Lett. **40**, 206 (1978).

[13] T. Munakata, Phys. Rev. A **45**, 1230 (1992).

[14] J. A. D. Wattis, Nonlinearity **9**, 1583 (1996).

[15] H. Frauenkron, Yu. S. Kivshar, and B. A. Malomed, Phys. Rev. E **54**, 2244 (1996).

[16] S. V. Dmitriev, T. Shigenari, A. A. Vasiliev, and A. E. Miroshnichenko, Phys. Lett. A **246**, 129 (1998).

[17] S. V. Dmitriev, T. Shigenari, A. A. Vasiliev, and K. Abe, Phys. Rev. B **55**, 8155 (1997).

[18] S. V. Dmitriev, L. V. Nauman, A. M. Wusatowska-Sarnek, and M. D. Starostenkov, Phys. Status Solidi B **201**, 89 (1997).

[19] B. V. Chirikov, Phys. Rep. **52**, 263 (1979).

[20] G. M. Zaslavsky, R. Z. Sagdeev, D. A. Usikov, and A. A. Chernikov, *Weak Chaos and Quasi-Regular Patterns* (Cambridge University Press, Cambridge, 1991).

[21] R. Hirota, J. Phys. Soc. Jpn. **33**, 1459 (1972).

[22] E. Hairer, S. P. Nörsett, and G. Wanner, *Solving Ordinary Differential Equations. Non-Stiff Problems* (Springer-Verlag, Berlin, 1993).